Electronic Supplementary Information (ESI) for:

Gas Adsorption in an Isostructural Series of Pillared Coordination Cages

Aeri J. Gosselin,[a,b,δ] Gregory R. Lorzing,[a,b,δ] Benjamin A. Trump,[c] Craig M. Brown,[c,d] Eric D. Bloch*[,a,b]

a. Department of Chemistry and Biochemistry, University of Delaware, Newark, Delaware 19716, United States

b. Center for Neutron Science, Department of Chemical and Biomolecular Engineering, University of Delaware, Newark, Delaware 19716, United States

c. Center for Neutron Research, National Institute of Standards and Technology, Gaithersburg, Maryland 20899, United States

d. Department of Chemical and Biomolecular Engineering, University of Delaware, Newark, Delaware 19716, United States

[δ]These authors contributed equally.

*edb@udel.edu

Chem. Commun.

Table of Contents

Experimental Section

General Considerations. All reagents were obtained from commercial vendors and used without purification, excluding solvents. Methanol was obtained from a solvent drying system and stored in a glove box under 3Å sieves. Thermogravimetric analyses (TGA) were carried out from 50°C to 600°C at a 2°C min^{-1} heating rate with a TA Q5000 SA under a nitrogen environment. All adsorption measurements were obtained on a Micromeritics 3Flex. Infrared spectroscopy was performed on a material using a Bruker Tensor 27 instrument. All samples were run in degassed paraffin oil. The paraffin oil was run as a background to be later subtracted from the IR spectra.

Neutron Diffraction

Neutron powder diffraction measurements were performed on 0.917 g Cu_bdc and 0.433 g Fe_bdc at the National Institute of Standards and Technology Center for Neutron Research (NCNR) using the high-resolution neutron powder diffractometer, BT1. Data was collected using Ge(311) monochromator with an in-pile 60' collimator, corresponding to a neutron wavelength of 2.0772 Å. Once transferred to a helium-purged glovebox, activated samples were placed into vanadium sample cans, and sealed with an indium O-ring onto a copper heating block containing a valved outlet for gas loading. The assembly was then mounted onto a bottom-loading closed cycle refrigerator (CCR) and connected to a gas manifold of a known volume.

Initial diffraction measurements were conducted at base temperature for the CCR (see Tables S1-S2). Fe_bdc was heated above 180 K to dose with C_2D_6 and C_2D_4. In between gases the sample was heated to 393 K while evacuating for 7 hours to ensure full reactivation. Full adsorption was verified barometrically before cooling to base temperature to avoid condensation of the vapor phase prior to the diffraction measurement.

X-ray Diffraction

All laboratory PXRD measurements except for Figure S6 were performed with a Bruker D8 XRD (LynxEye position sensitive detector) operating with a Cu Kα1 x-ray generator (λ=1.54Å) with a 40 kV beam voltage and 40 mA current. Diffraction patterns shown in Figure S6 were collected on a Bruker-AXS APEX II DUO CCD diffractometer with Cu-Kα radiation (λ = 1.54 Å).

Synchrotron powder X-ray diffraction measurements were performed on Cu_OH-bdc at the Advanced Photon Source, Argonne National Laboratory, using beamline 17-BM-B. Data was collected using a 2-D Si-plate detector with an incident wavelength of 0.45220 Å. Prior to measurement samples were loaded into 1 mm quartz capillaries and sealed with wax in a nitrogen glovebox.

Laboratory powder X-ray diffraction measurements were collected using Cu Kα radiation (λ_{avg} = 1.5418 Å) on a Bruker D8 Discover diffractometer with a LynxEye detector. Fe_OH-bdc sample was loaded in a quartz capillary prior to measurement in a nitrogen glovebox.

Structure Solution

Neutron and X-ray diffraction data was analyzed using Topas Academic.[1] The space group (*Fm*-3*m*) and initial unit cell were chosen based on the analogous previously reported Co and Zn compounds.[2] More precise lattice parameters, peak shapes, and background function were determined by a Pawley refinement.[3] Where possible, the crystal structures were then solved by the global optimization method of simulated annealing (SA) in real space.[4]

For the SA refinements, a full isophthalic acid (ip^{2-}, bdc) (with respective H- or hydroxy- groups) was centered and refined on a 96*k* (*x*, *x*, *z*) position and allowed to rotate using one variable to ensure the molecule overlapped with itself. The dabco molecule was refined on a 48*i* (*x*, 0.5, -*x*) position and allowed to rotate around a fixed axis using one degree of freedom. An additional ip^{2-} and DMF molecules were added and refined while centered on a 96*k* (*x*, *x*, *z*) and a 32*f* (*x*, *x*, *x*) position respectively. The additional ip^{2-} was allowed to freely rotate while DMF rotated around a fixed axis using one degree of freedom. After a reasonable structure was determined the internal degrees of freedom for each molecule was additionally refined. Finally, the number of atoms and their Wyckoff positions were corrected, then occupancies and thermal parameters were refined. Occupancies that refined within error of unity were fixed.

For SA refinements involving extra gas molecules, the initial structure was fixed while freely refining a single gas molecule. Fourier difference maps could not be utilized to determine initial positions due to the amount of disordered solvent molecules and the likelihood of competitive adsorption displacing them. Once initial gas molecules positions were determined, two molecules were allowed to freely rotate on the a 96*k* (*x*, *x*, *z*) and a 32*f* (*x*, *x*, *x*) Wyckoff positions.

Some structures were unable to achieve suitable Rietveld refinements due to either additional disordered solvent molecules or structural deformities. Figure S1 displays that a *Fm*-3*m* space group fits most of the reflections for Fe_OH-bdc, however there is a peak $2\theta \approx 16.5°$ that is not fit with a cubic space group. Alternatively, trigonal space group *P*-3 does fit this reflection, shown in Figure S2. As no known secondary phases account for this peak, this indicates that the symmetry is lowered, possibly due to deformity of the MOF framework.

Due to Cu_OH-bdc decomposing upon activation, a Rietveld refinement was attempted for the solvated structure. Space group *Fm*-3*m* models the data quite well, however several broad, low-angle features are observed ($2\theta \approx 1°$, $\approx 1.8°$, $\approx 2°$), as shown in Figure S6. Despite these discrepancies, a Rietveld refinement also models the data quite well (seen in Figure S7), however the model contains only one extra DMF and one extra bdc linker. Seeing as this material was not activated at all, it likely contains even more disordered molecules, which explains the discrepancies with the refinement in the $2\theta = 1.2°$-$1.4°$ range. Similarly, due to the high level of molecular overlap and symmetry restrictions on disordered molecules their modelled positions may be inaccurate.

Table S1: Crystallographic parameters for Cu-iso, Fe-iso, and Fe-me using *Fm*-3*m* (225) obtained from Rietveld refinements to neutron powder diffraction data. Values given in parentheses represent one standard deviation.

	Cu-bdc	Cu-OH-bdc	Fe-bdc
a (Å)	39.942(3)	39.977(14)	40.302(2)
V (Å^3)	63722(5)	63887(7)	65460(3)
T (K)	7.05(4)	298.0(2)	12.1(1)
R_{wp} (%)	2.810	9.477	3.310
R_p (%)	2.445	6.857	2.865
R_{exp} (%)	2.460	3.550	3.123
χ^2 (%)	1.142	2.670	1.060

*Values taken from Pawley refinements.

$$R_p = \sqrt{\frac{\sum |Y_{o,m} - Y_{c,m}|}{\sum Y_{o,m}}}$$

$$R_{wp} = \sqrt{\frac{\sum w_m \left(Y_{o,m} - Y_{c,m}\right)^2}{\sum w_m Y_{o,m}^2}}$$

$$R_{exp} = \sqrt{\frac{\sum M - P}{\sum w_m Y_{o,m}^2}}$$

$$\text{GoF} = \chi^2 = \sqrt{\frac{\sum w_m \left(Y_{o,m} - Y_{c,m}\right)^2}{M - P}}$$

Table S2: Crystallographic parameters for C_2D_4 and C_2D_6 dosed Fe-iso using *Fm*-3*m* (225) obtained from Rietveld refinements to neutron powder diffraction data. Values given in parentheses represent one standard deviation.

Fe-iso	C_2D_4	C_2D_6
a (Å)	40.216(3)	40.251(3)
V (Å^3)	65042(5)	65212(5)
T (K)	12.1(1)	12.1(1)
R_{wp} (%)	3.852	3.813
R_p (%)	3.305	3.413
R_{exp} (%)	3.570	3.346
GoF (%)	1.079	1.139
amt. per f.u.	1.88(4)	1.48(3)

Synthetic Techniques

Synthesis of Cu_bdc_dabco. $Cu(NO_3)_2 \cdot 2.5H_2O$ (0.116 g, 0.50 mmol), benzene-1,3-dicarboxylic acid (H_2BDC) (0.083 g, 0.50 mmol), ethanol (3 mL), and N,N'-dimethylacetamide (15 mL) were added to a 20 mL scintillation vial and sealed with a Teflon lined cap. The resulting solution was then heated in an oven at 365 K. After one hour 1,4-diazabicyclo[2.2.2]octane (DABCO) (0.056 g, 0.50 mmol) was added to the hot reaction mixture and the solution heated for an additional 24 hours. A light blue precipitate was isolated via vacuum filtration with care taken to avoid filtering the product to compete dryness. Solvent exchange was completed by soaking the product in fresh DMA at 373 K for three days with the solvent replaced every 12 hours. The DMA washed solid was isolated by centrifugation and soaked in chloroform at 333 K for three days with the solvent replaced every 12 hours. Activated material was obtained by flowing nitrogen over the sample for 48 hours followed by evacuation at 348 K.

Synthesis of Fe_bdc_dabco. In an N_2 glovebox, $FeCl_2$ (0.150 g, 1.183 mmol) and H_2BDC (0.200 g, 1.204 mmol) were dissolved in DMF (12 mL) in a capped 20 mL scintillation vial and heated at 393 K for two hours. DABCO (0.132 g, 1.177 mmol) was then dissolved in methanol (1.85 mL) and added to the DMF solution. The resulting mixture was heated at 343 K for 48 hours. The resulting fluffy yellow solid was removed from the vial by pasteur pipette-tip filtration with care taken to avoid the collection of large dark yellow-orange crystals that occasionally form. The light-yellow solid was isolated by centrifugation and soaked in DMF at room temperature for three days replacing the solvent with fresh DMF every 8 hours. After DMF washing the solid was washed with benzene by a similar procedure. Over the course of benzene washes, the solid turns a lime-green color. Activated material was obtained by evacuation of frozen benzene at 273 K for two days followed by heating under vacuum at 323 K for two days. The resulting light green solid is incredibly air sensitive, turning dark brown upon exposure to O_2.

Synthesis of Co_bdc_dabco. In a 100mL VWR Media Bottle, $CoCl_2$ (2.365 g, 9.941 mmol), and H_2BDC (1.676 g, 10.091 mmol) were dissolved in DMF (100 mL) and left to sit at room temperature for five days. In a separate 100 mL VWR Media Bottle, DABCO (1.122 g, 10.007 mmol), was dissolved in DMF (100 mL). The resulting cobalt/ligand stock solution (10 mL) was pipetted into a PTFE Sampling Bottle. DABCO solution (10 mL) was layered onto the cobalt/ligand solution. The resulting solution was capped and heated at 373 K for 12 hours. The sample was allowed to cool to room temperature before removing excess solvent. Resulting dark green cubic crystals were removed from the bottle with fresh DMF and a Pasteur pipette. Solvent exchange was completed by soaking the product in fresh DMF at 383 K for 3 days with the solvent replaced every 12 hours. The DMF washed solid was isolated by removing excess solvent with a Pasteur pipette and then soaked in chloroform at 333 K for three days with the solvent replaced every 12 hours. Activated material was obtained by evacuation at 348 K. A Langmuir surface area of 2,372 m^2/g was obtained.

Synthesis of Cu_OH-bdc_dabco. This synthesis was adapted from Li, J. R.; Zhou, H. *Nat. Chem.* 2010, *2*, 893-898. $Cu(NO_3)_2 \cdot H_2O$ (0.605 mg, 2.6 mmol), 5-hydroxy-1,3-dicarboxylic acid (H_2Me-BDC) (0.458 g, 2.5 mmol), methanol (75 mL), N,N'-dimethylacetamide and 10 drops of 2,6-Lutidene were added to a 100 mL VWR glass jar. The solution was allowed to sit at room temperature for seven days. This afforded blue crystals of metal-organic polyhedra. Polyhedra crystals were collected and devoid of solvent via pipet. Copper hydroxy polyhedra (120 mg) were dissolved in methanol (1 mL) in a 20 mL scintillation vial. N'N-dimethylformamide (9 mL) and 1,4-diazabicyclo[2.2.2]octane (DABCO) (45 mg, 0.4 mmol) were added to the solution. The resulting solution was heated at 363 K for seven hours. A light green precipitate was isolated via vacuum filtration with care taken to avoid filtering the product to complete dryness.

Digestion of Materials for ^{1}H-NMR. Cu_bdc_dabco powders were digested in DCl (35% wt in D_2O). The resulting solution (0.1 mL) and DMSO-d_6 (0.7 mL) were combined in a 4 mL scintillation vial and swirled until all solid dissolved.[5] ^{1}H-NMR spectra were taken on a AV 400 spectrometer equipped with a cryogenic QNP probe.

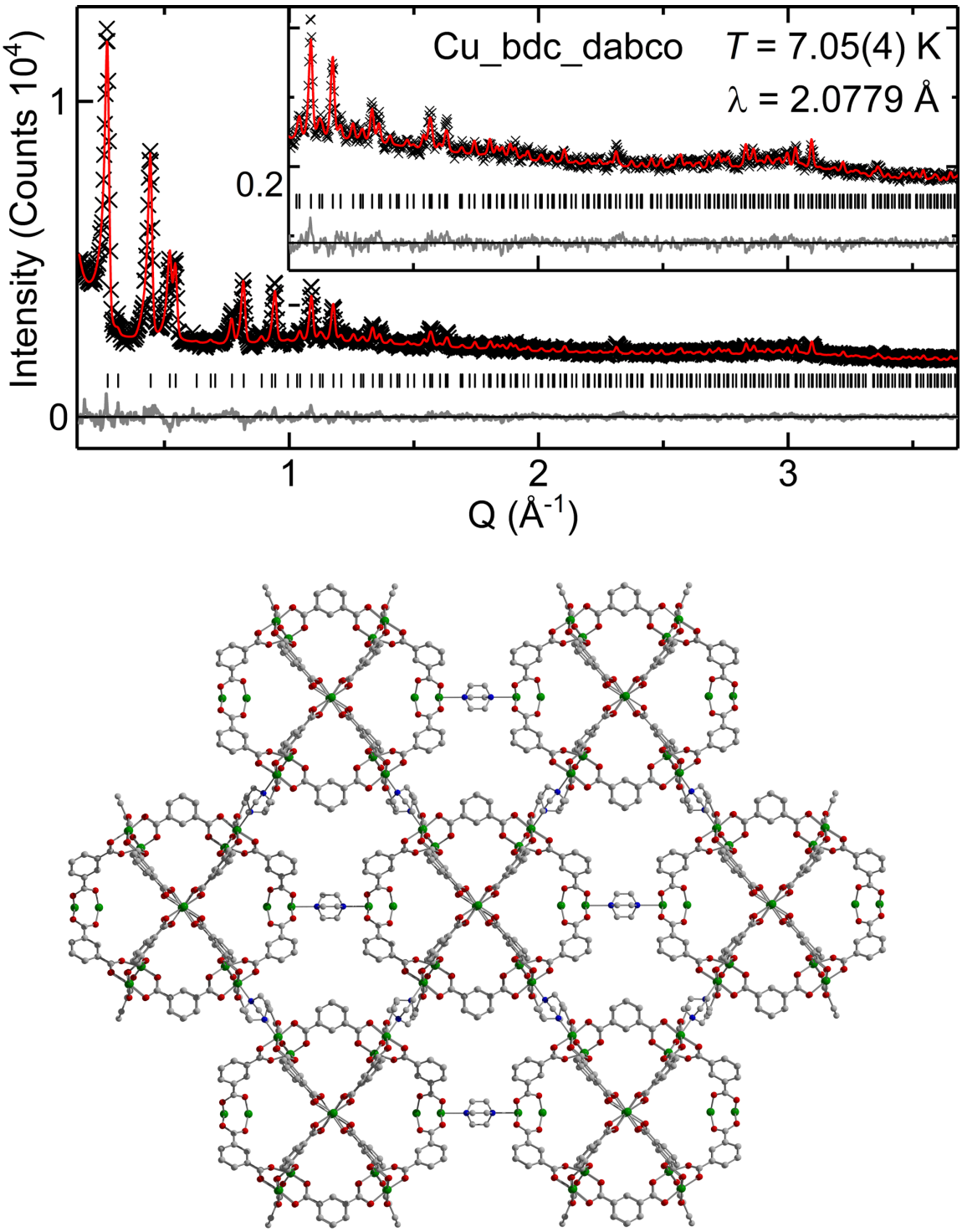

Figure S1. (Upper) Rietveld refinement of activated Cu_bdc_dabco, using *Fm-3m* unit cell with $a = b = c =$ 39.94(3) at 7.1 K. (Below) Corresponding structure of Cu_bdc_dabco. Green, gray, blue and red represent copper, carbon, nitrogen and oxygen respectively.

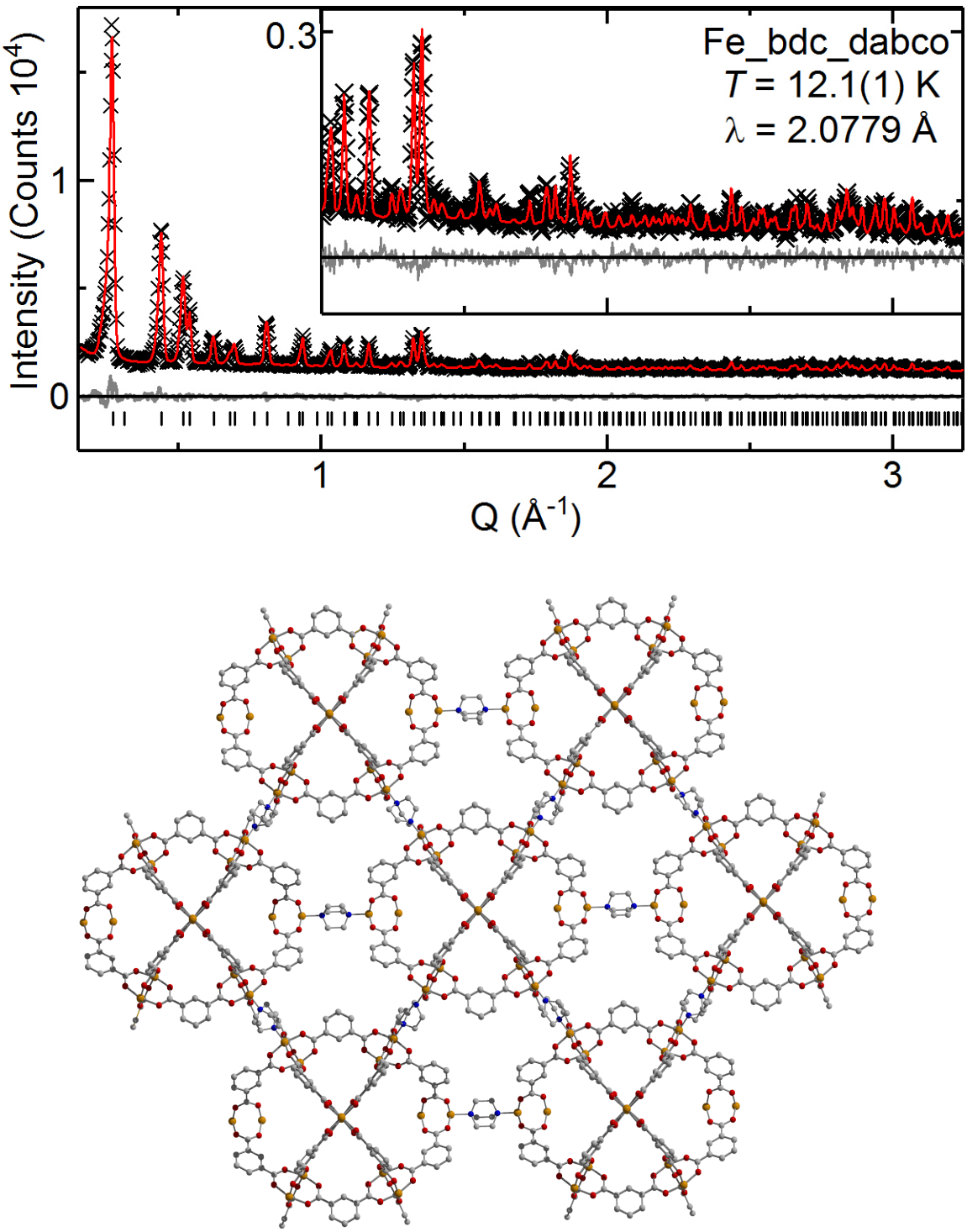

Figure S2. (Upper) Rietveld refinement of activated Fe_bdc_dabco, using *Fm-3m* unit cell with $a = b = c =$ 40.302(2) at 12.1 K. (Below) Corresponding structure of Fe_bdc_dabco. Orange, gray, blue and red represent iron, carbon, nitrogen and oxygen respectively.

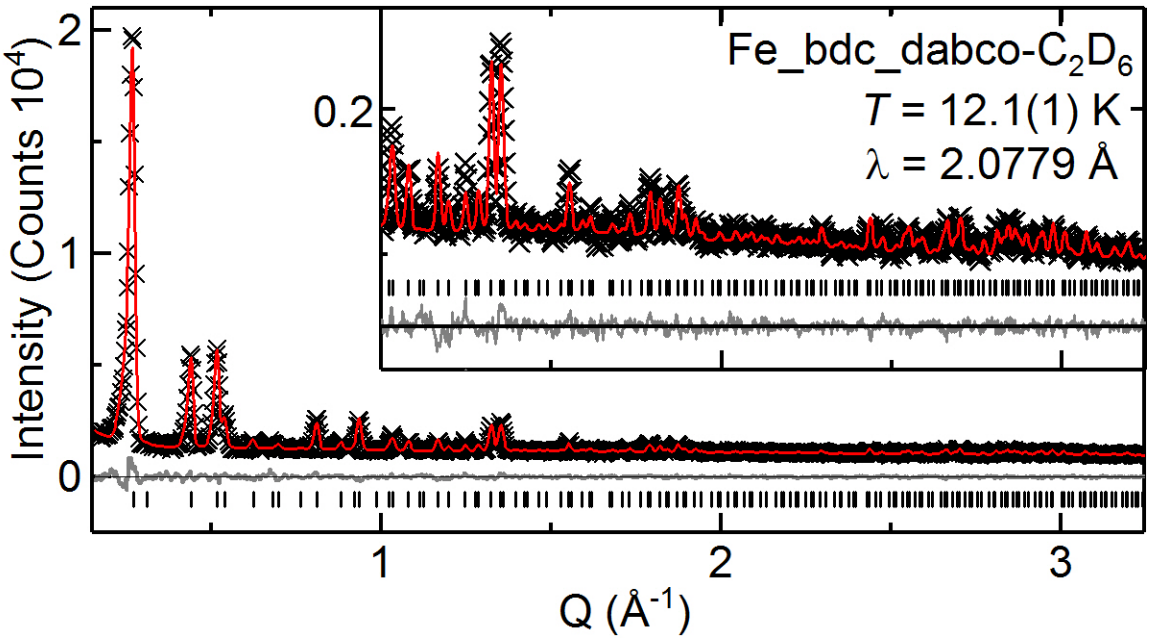

Figure S3. Rietveld refinement of Fe_bdc_dabco dosed with ethane.

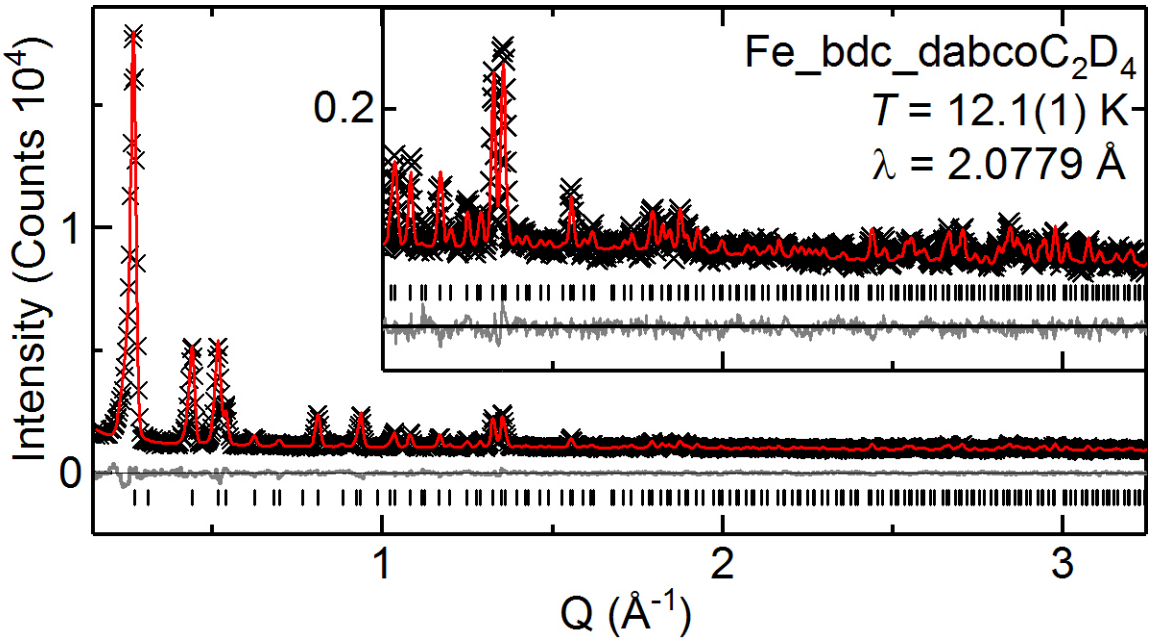

Figure S4. Rietveld refinement of Fe_bdc_dabco dosed with ethylene.

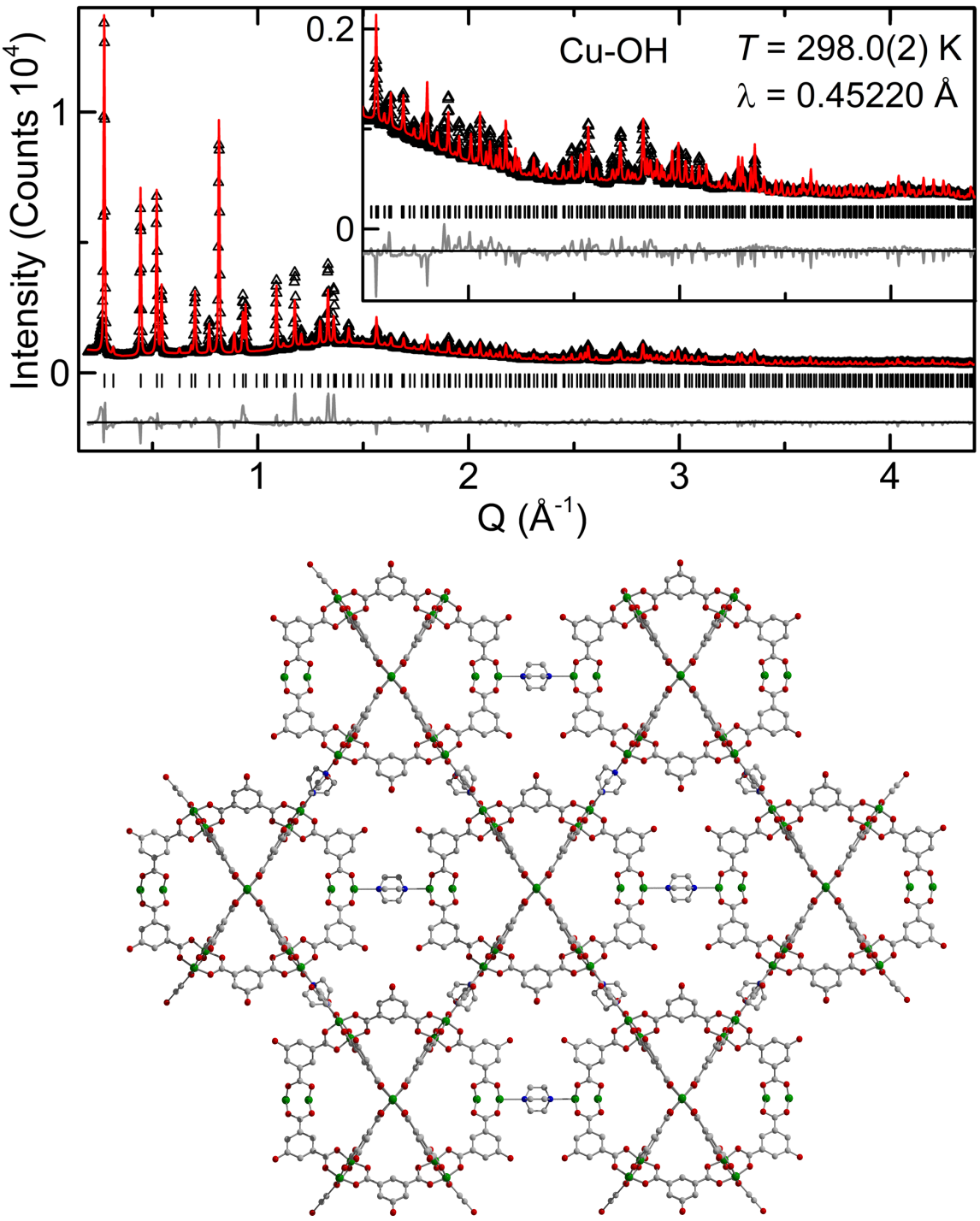

Figure S5. (Upper) Rietveld refinement of Cu_OH-bdc synchrotron powder X-ray diffraction data using space group *Fm*-3*m* (black ticks, *a* = 39.977(14)). Experimental data shown as black triangles, fit in red, with difference curve in gray. Symbols are commensurate with error bars. (Below) Corresponding structure of Cu_OH-bdc_dabco. Green, gray, blue and red represent copper, carbon, nitrogen and oxygen respectively.

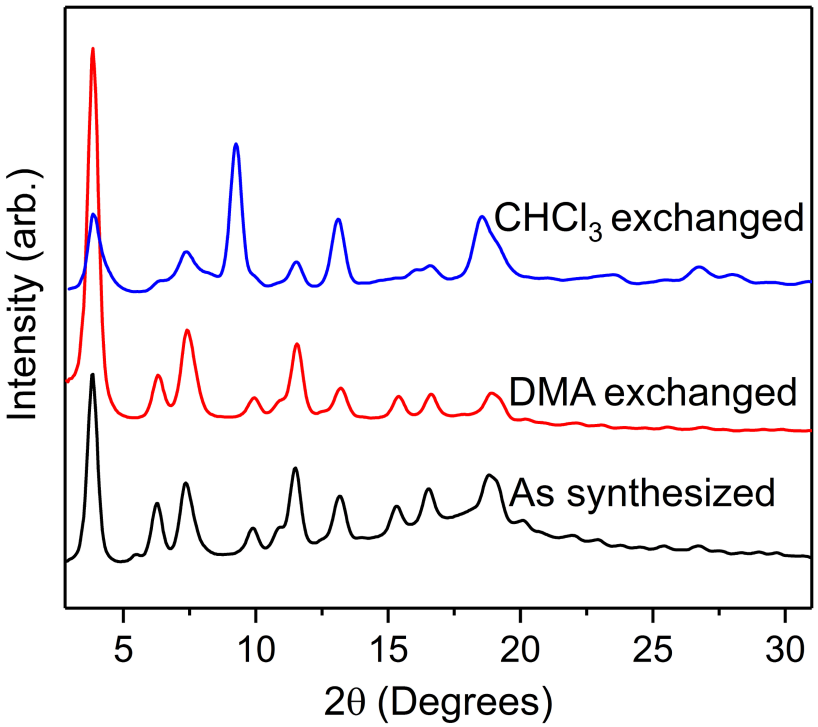

Figure S6. Powder X-ray diffraction patterns of Cu_bdc_dabco DMA exchanged (red), chloroform exchanged (blue), and activated (green).

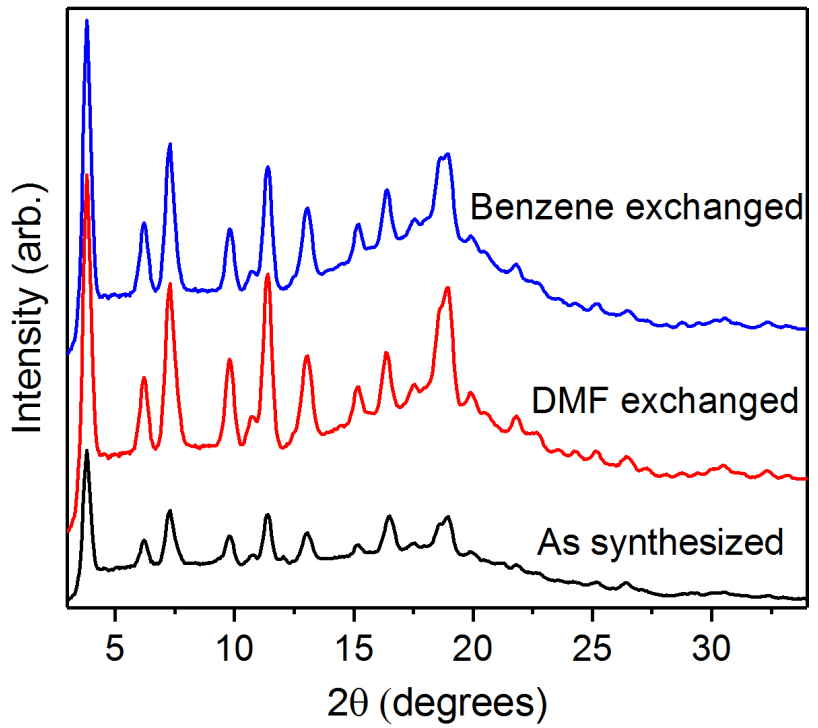

Figure S7. Powder X-ray diffraction pattern of Fe_bdc_dabco as synthesized (black), DMF exchanged (red) and benzene exchanged (blue).

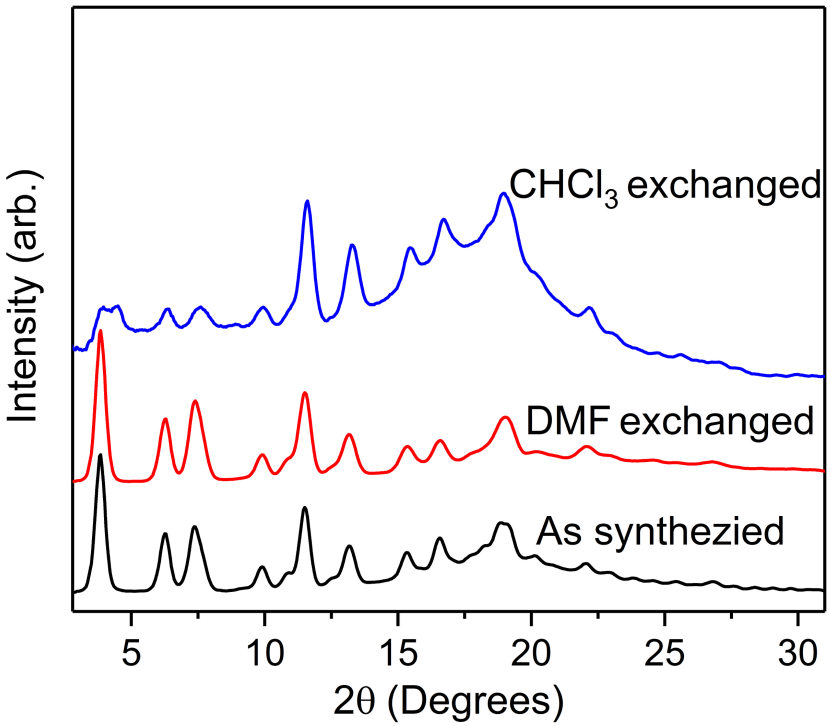

Figure S8. Powder X-ray diffraction patterns of Cu_OH-bdc_dabco DMA exchanged (red) and chloroform exchanged (blue).

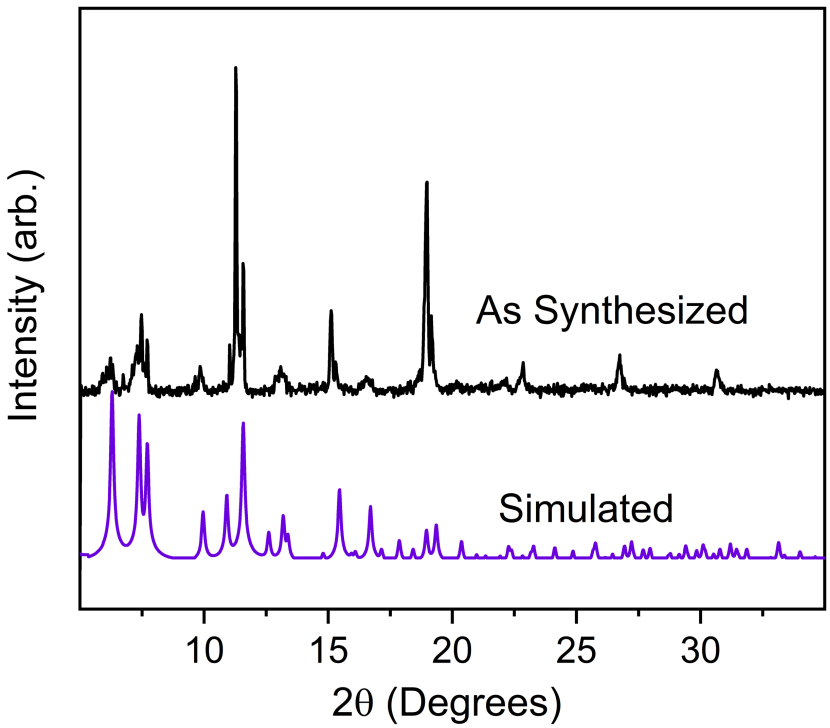

Figure S9. Powder X-ray diffraction pattern of Co_bdc_dabco as synthesized (black) and simulated (purple).

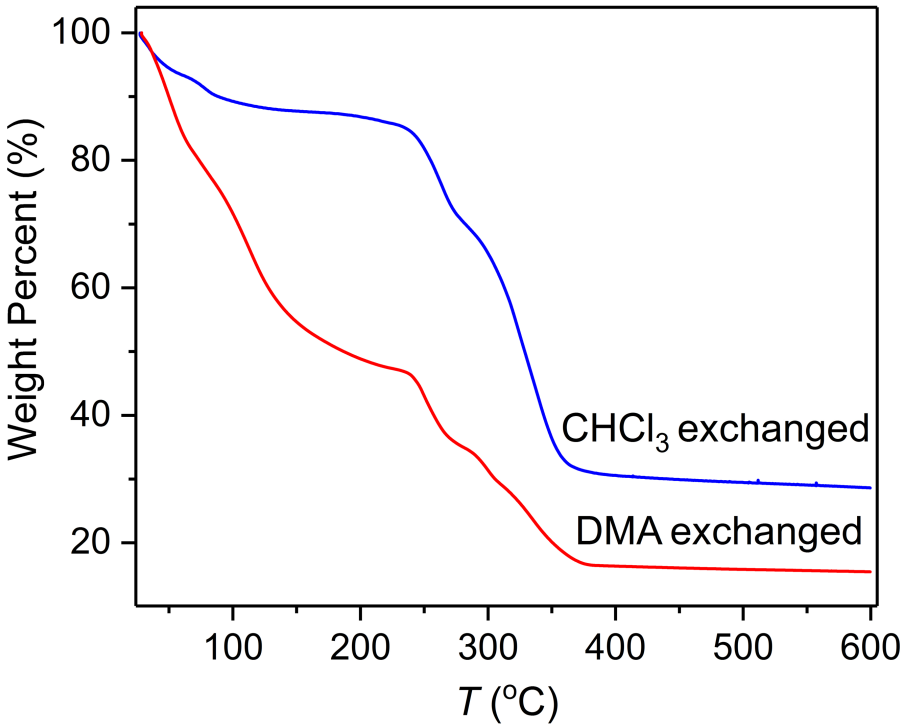

Figure S10. Thermogravimetric analysis of DMA exchanged (red) and $CHCl_3$ exchanged (blue) Cu_bdc_dabco from RT to 600 °C at a ramp rate of 2 degrees per minute.

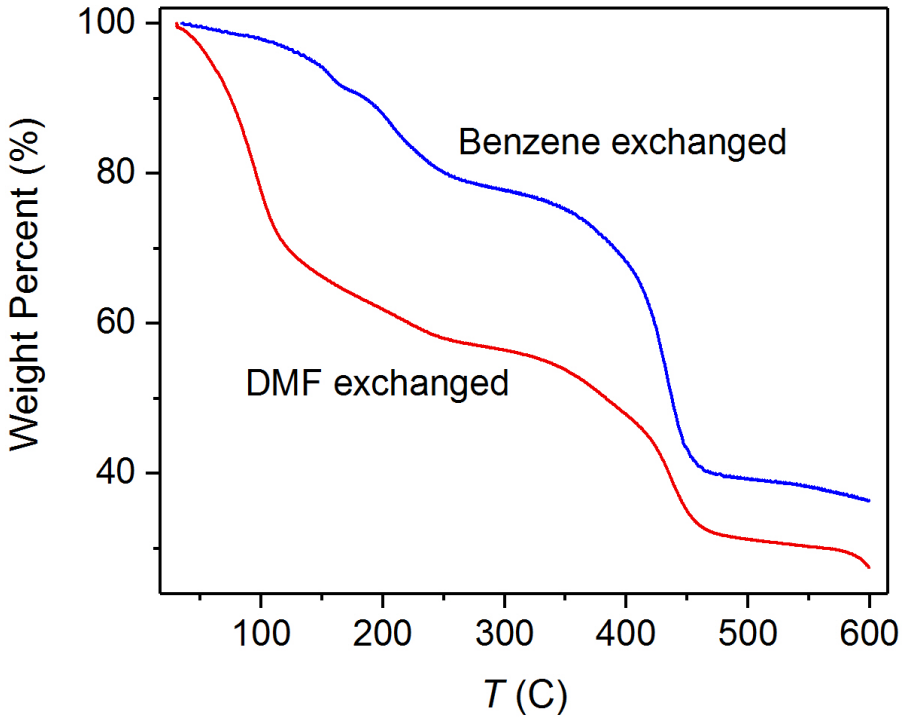

Figure S11. Thermogravimetric analysis of DMF exchanged (red) and benzene exchanged (blue) Fe_bdc_dabco from 50 °C to 600 °C at a ramp rate of 2 degrees per minute.

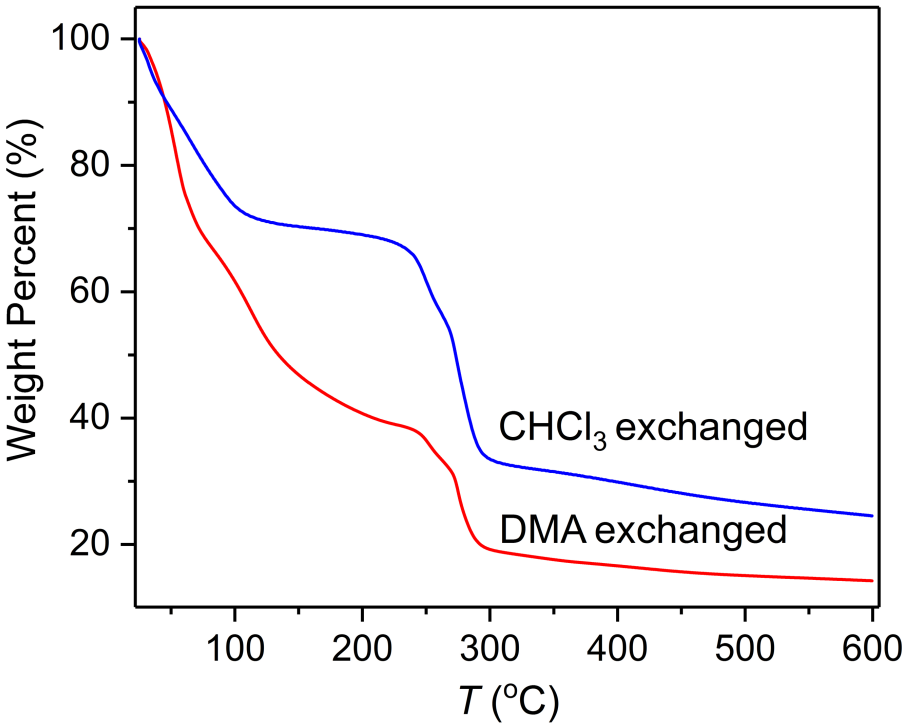

Figure S12. Thermogravimetric analysis of DMA exchanged (red) and $CHCl_3$ exchanged (blue) Cu_OH-bdc_dabco from 50 °C to 600 °C at a ramp rate of 2 degrees per minute.

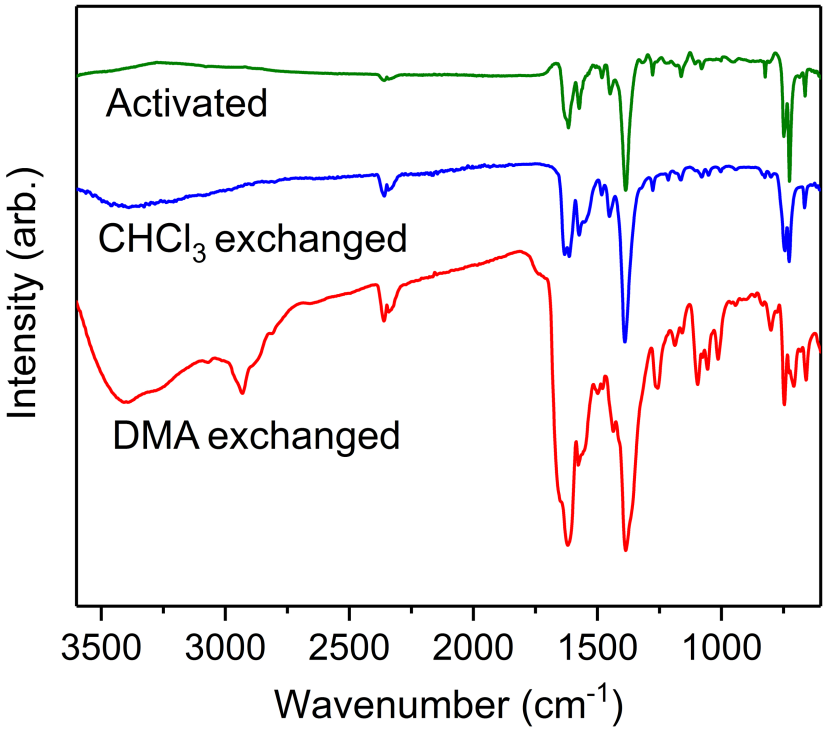

Figure S13. IR spectra of Cu_bdc_dabco DMA exchanged (red), chloroform exchanged (blue), and activated (green).

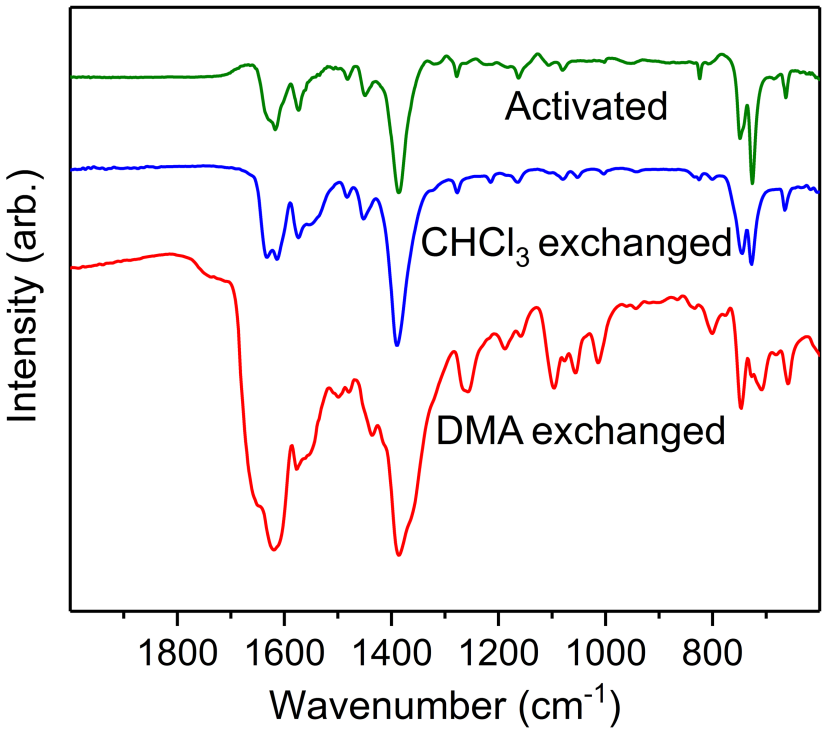

Figure S14. IR spectra of Cu_bdc_dabco DMA exchanged (red), chloroform exchanged (blue), and activated (green).

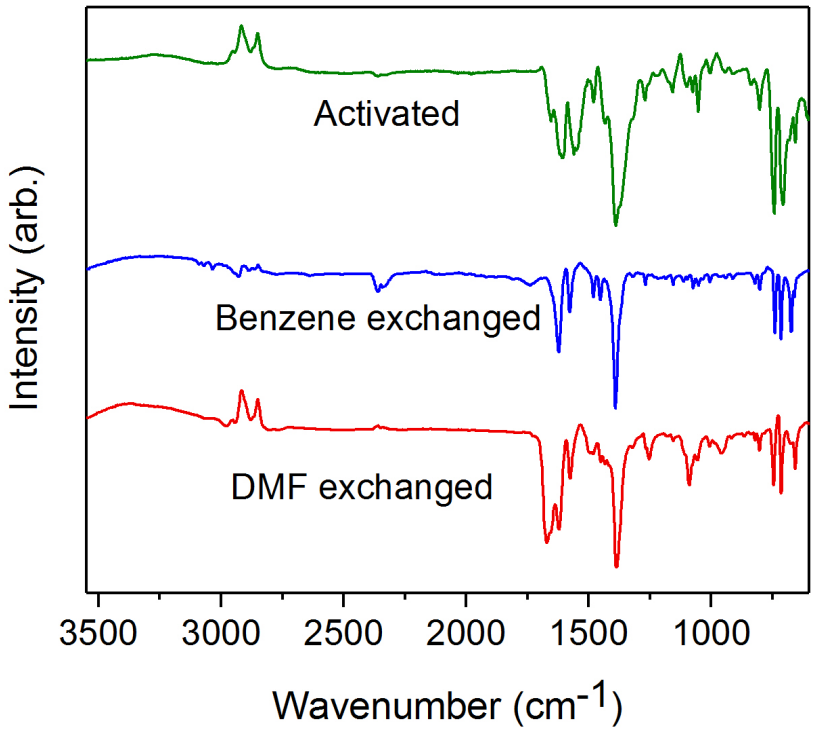

Figure S15. IR spectra of Fe_bdc_dabco as DMF exchanged (red), benzene exchanged (blue), and activated (green).

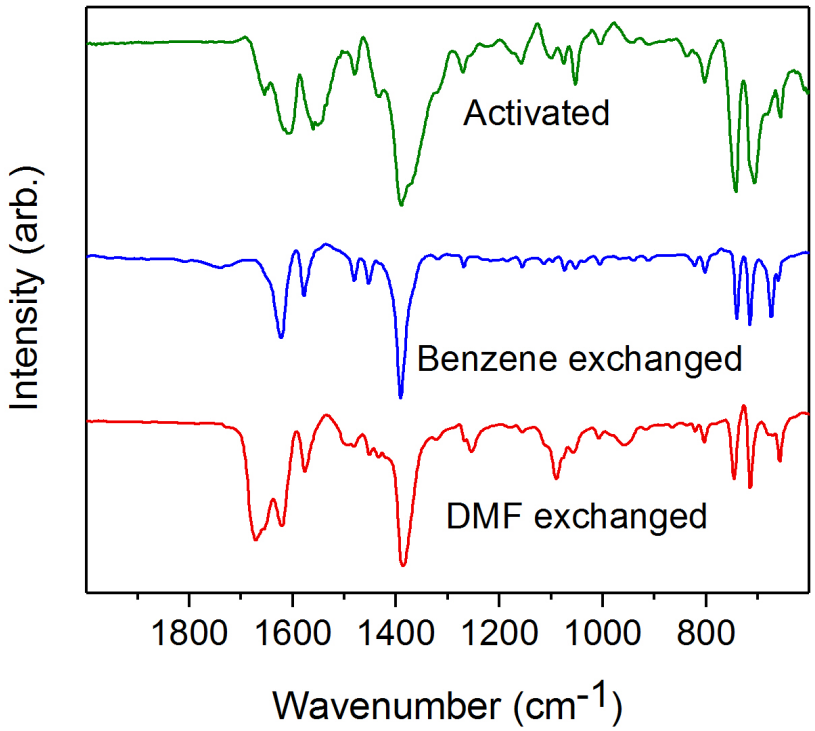

Figure S16. IR spectra of Fe_bdc_dabco as DMF exchanged (red), benzene exchanged (blue), and activated (green).

Gas Adsorption Measurements

All gas adsorption measurements were obtained with a Micromeritics 3Flex gas adsorption analyzer. The 3Flex tubes were evacuated on the Smartvac system after being heating in the oven to remove water. Once cooled and evacuated, the sealed tubes were weighed and then brought into the glove box. The M_bdc_dabco samples were loaded into the tubes, sealed, removed from the glove box and degassed at room temperature for 12h. The Cu_bdc_dabco sample was heated to 25 °C at a ramp of 2 °C/min. Fe_bdc_dabco was heated to 50 °C at a ramp of 2 °C/min.Each sample was considered activated when the static outgas rate was less than 2 μbar/min. Once fully activated, the tube was weighed to determine an accurate mass of the sample. Surface areas and pore volumes were measured via N_2 isotherm in a 77 K liquid nitrogen bath and calculated using the Micromeritics software. All other isotherms were collected by submerging the entire sample tube in a temperature controlled water bath.

Fitting of Isotherms

The adsorption isotherms were fit with single or dual-site Langmuir-Freundlich model (Eqn. 1), where n is the absolute amount adsorbed in mmol/g, P is the pressure in bar, $q_{sat,i}$ is the saturation capacity in mmol/g, b_i is the Langmuir parameter in bar^{-1}, and v_i is the Freundlich parameter for two sites 1 and 2. The parameters used to fit the adsorption isotherms can be found in Tables S3-S11. Plots of the adsorption isotherms along with their fits are presented in Figures S21-S29.

$$n = \frac{q_{sat,1} b_1 P^{v_1}}{1+b_1 P^{v_1}} + \frac{q_{sat,2} b_2 P^{v_2}}{1+b_2 P^{v_2}} \quad (1)$$

The isosteric heats of adsorption, $-Q_{st}$, were calculated through the use of the Clausius-Clapeyron equation (Eqn 2) for each gas using single or dual-site Langmuir-Freundlich fits for each material at 298 K, 308 K, and 318 K. P is the pressure, n is the amount adsorbed, T is the temperature, R is the universal gas constant, and C is a constant. Based on plots of $(\ln P)_n$ as a function of $1/T$ the isosteric heat adsorption was obtained by the slope. The isosteric heat of adsorption for each gas is shown in Figure S21.[6]

$$\ln P = -\frac{Q_{st}}{R}\left(\frac{1}{T}\right) + C \quad (2)$$

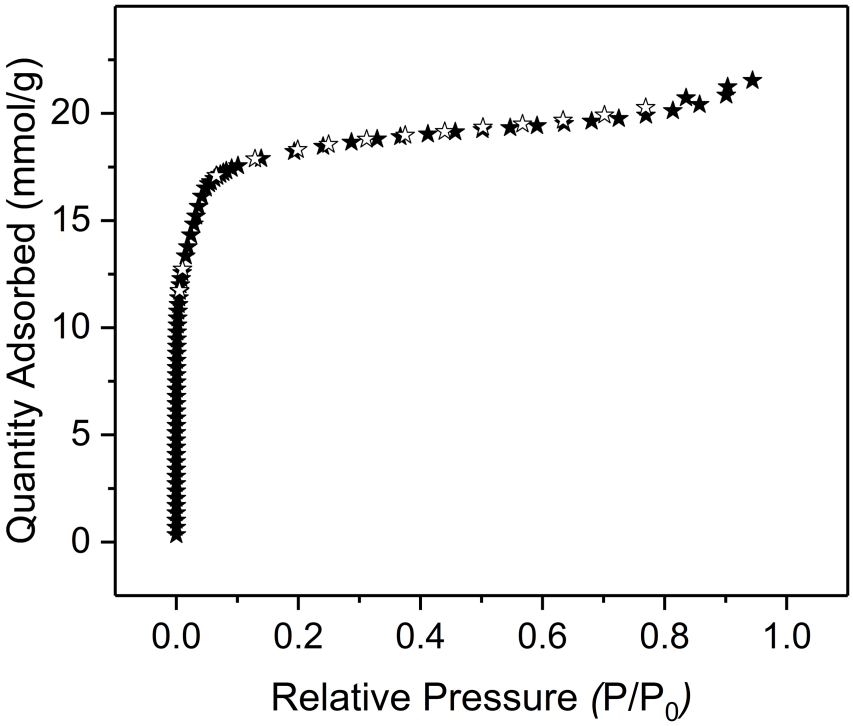

Figure S17. N_2 adsorption in Cu_bdc_dabco at 77 K. Closed symbols and open symbols represent adsorption and desorption, respectively.

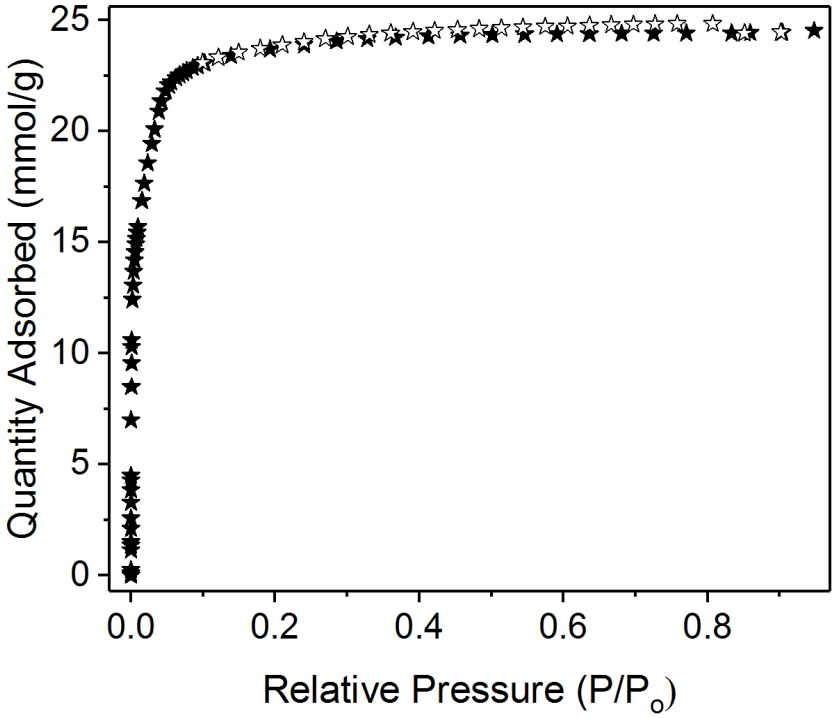

Figure S18. N_2 adsorption in Fe_bdc_dabco at 77 K. Closed symbols and open symbols represent adsorption and desorption, respectively.

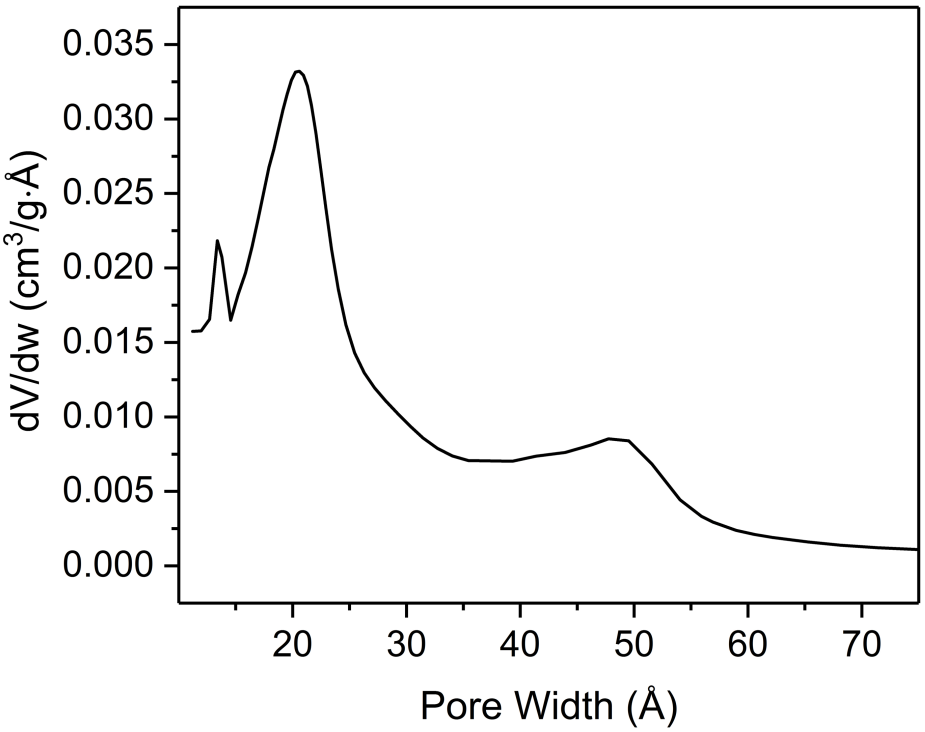

Figure S19. Pore size distribution in Cu_bdc_dabco calculated from N_2 adsorption at 77 K.

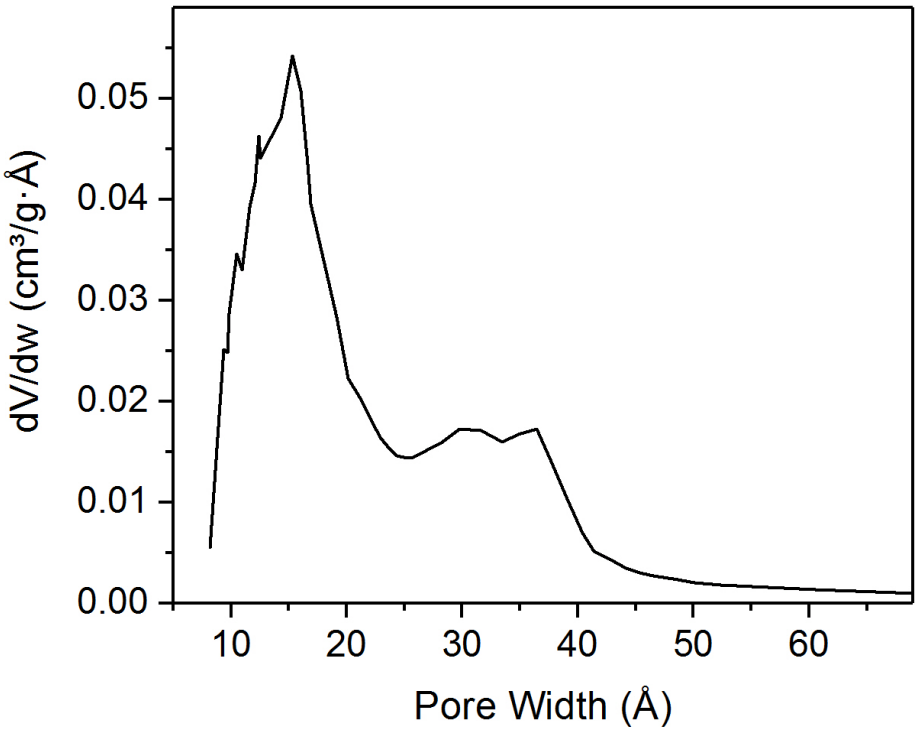

Figure S20. Pore size distribution in Fe_bdc_dabco calculated from N_2 adsorption at 77 K.

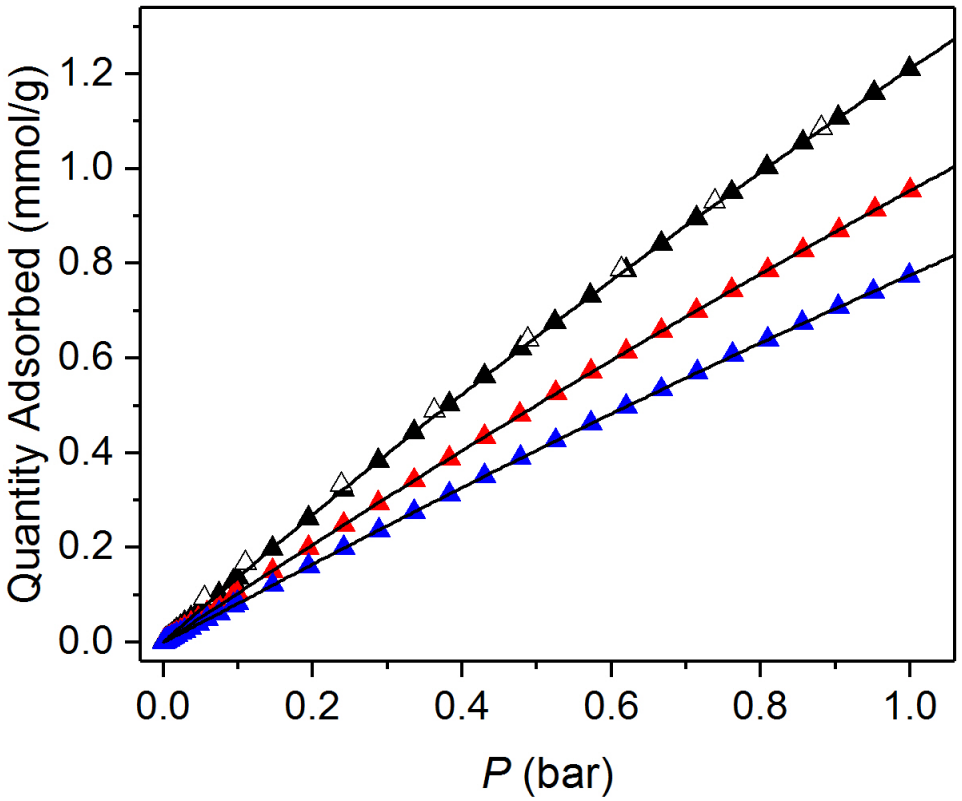

Figure S21. Pure component isotherm data for carbon dioxide in Fe_bdc_dabco. The black triangles refer to 298 K, red for 308 K, and blue for 318 K. The closed triangles show adsorption data while the open triangles show desorption. The black lines are the respective single-site Langmuir-Freundlich fits using the parameters in Table S3.

Table S3.

	298 K	**308 K**	**318 K**
$q_{sat,1}$ (mmol/g)	10.247 ± 0.138	8.946 ± 0.239	6.545 ± 0.251
b_1 (bar)	0.134 ± 0.002	0.119 ± 0.004	0.134 ± 0.001
v_1	0.996 ± 0.001	1.009 ± 0.002	1.026 ± 0.003

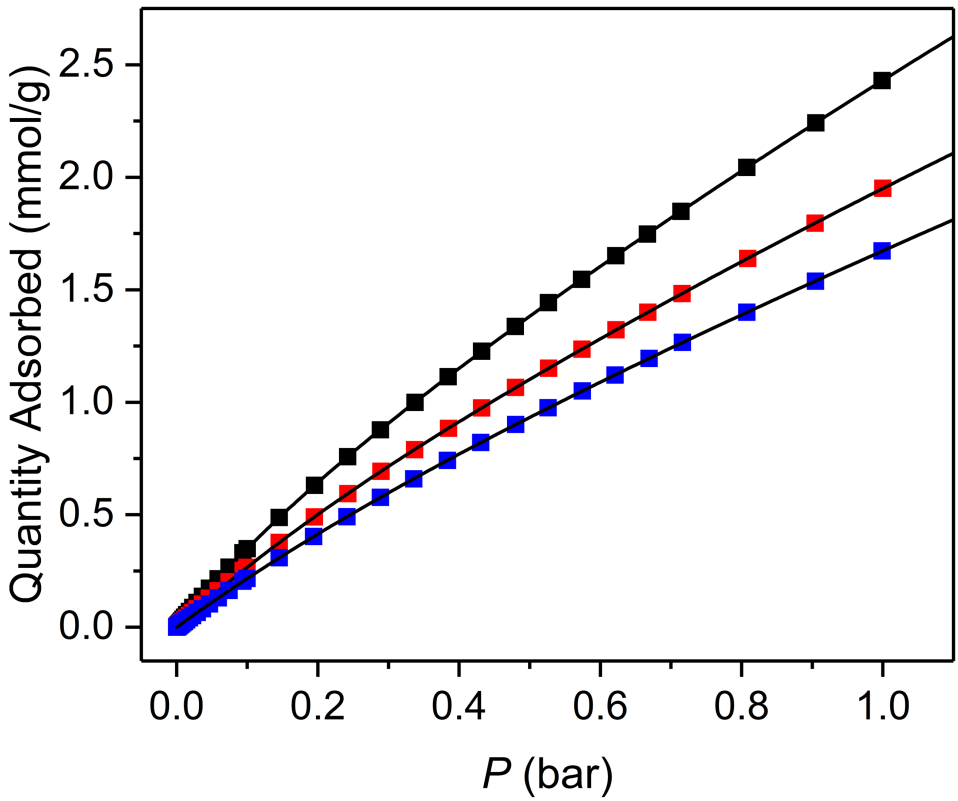

Figure S22. Pure component isotherms data for ethane in Fe_bdc_dabco. The black squares refer to 298 K, red for 308 K, and blue for 318 K. The closed squares show adsorption data while the open squares show desorption. The black lines are the respective dual-site Langmuir-Freundlich fits using the parameters in Table S4.

Table S4.

	298 K	**308 K**	**318 K**
$q_{sat,1}$ (mmol/g)	2.225 ± 0.001	2.805 ± 2.097	3.443 ± 3.687
b_1 (bar)	1.552 ± 0.008	0.965 ± 0.636	0.644 ± 0.647
v_1	0.970 ± 0.001	0.982 ± 0.015	0.989 ± 0.013
$q_{sat,2}$ (mmol/g)	7.224 ± 0.005	4.636 ± 6.624	4.809 ± 13.993
b_2 (bar)	0.175 ± 0.001	0.141 ± 0.072	0.072 ± 0.081
v_2	1.583 ± 0.005	1.789 ± 0.846	1.929 ± 1.504

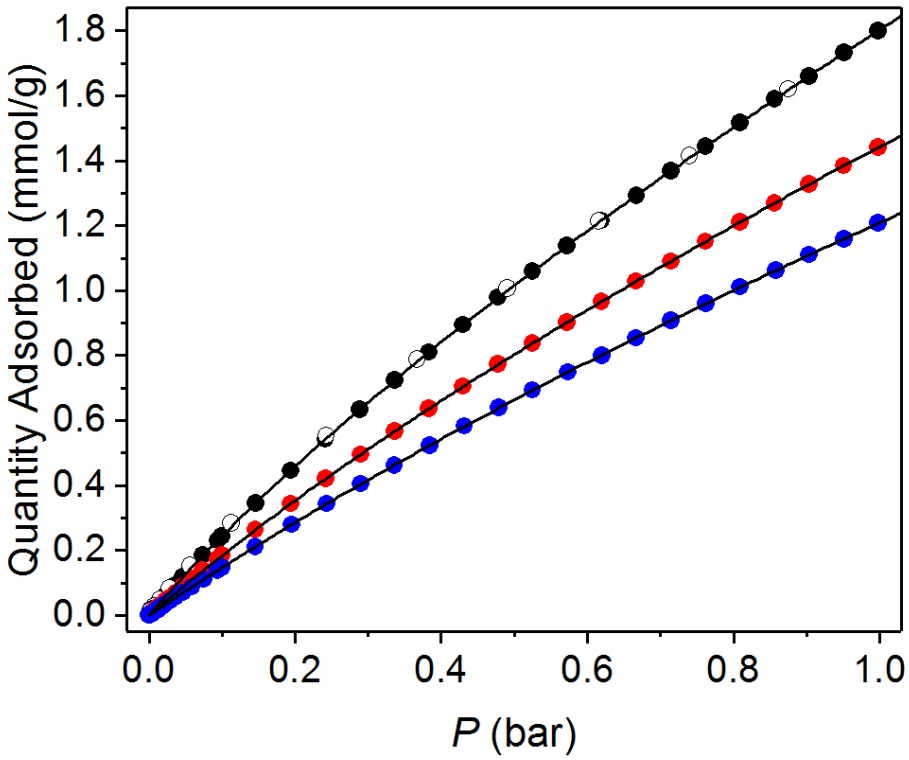

Figure S23. Pure component isotherms data for ethylene in Fe_bdc_dabco. The black circles refer to 298 K, red for 308 K, and blue for 318 K. The closed circles show adsorption data while the open circles show desorption. The black lines are the respective dual-site Langmuir-Freundlich fits using the parameters in Table S5.

Table S5.

	298 K	**308 K**	**318 K**
$q_{sat,1}$	3.063 ± 2.076	3.227 ± 3.618	4.0983 ± 3.428
b_1	0.806 ± 0.526	0.591 ± 0.655	0.375 ± 0.324
v_1	0.982 ± 0.005	0.995 ± 0.003	1.000 ± 0.091
$q_{sat,2}$	2.919 ± 3.819	1.676 ± 4.352	0.600 ± 2.155
b_2	0.175 ± 0.067	0.171 ± 0.108	0.192 ± 0.299
v_2	1.939 ± 0.796	2.066 ± 1.45	2.465 ± 1.979

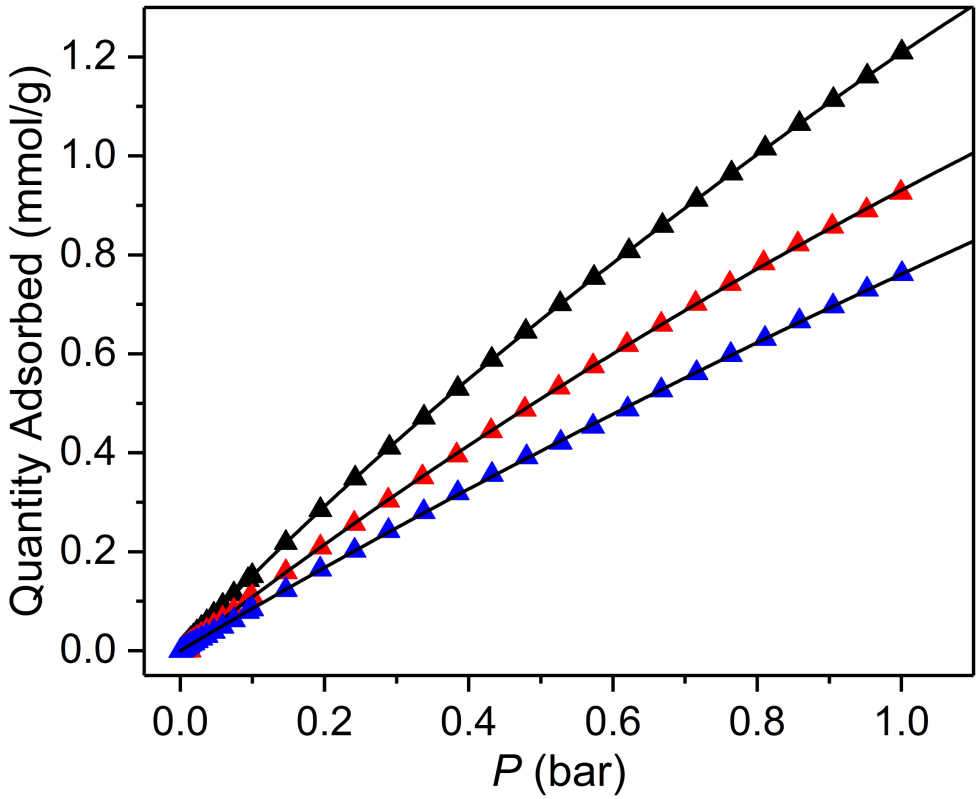

Figure S24. Pure component isotherm data for carbon dioxide in Co_bdc_dabco. The black triangles refer to 298 K, red for 308 K, and blue for 318 K. The closed triangles show adsorption data while the open triangles show desorption. The black lines are the respective single-site Langmuir-Freundlich fits using the parameters in Table S6.

Table S6.

	298 K	**308 K**	**318 K**
$q_{sat,1}$	6.353 ± 0.288	5.004 ± 0.195	7.223 ± 0.818
b_1	0.231 ± 0.012	0.229 ± 0.011	0.118 ± 0.015
v_1	0.974 ± 0.002	1.012 ± 0.005	0.993 ± 0.007

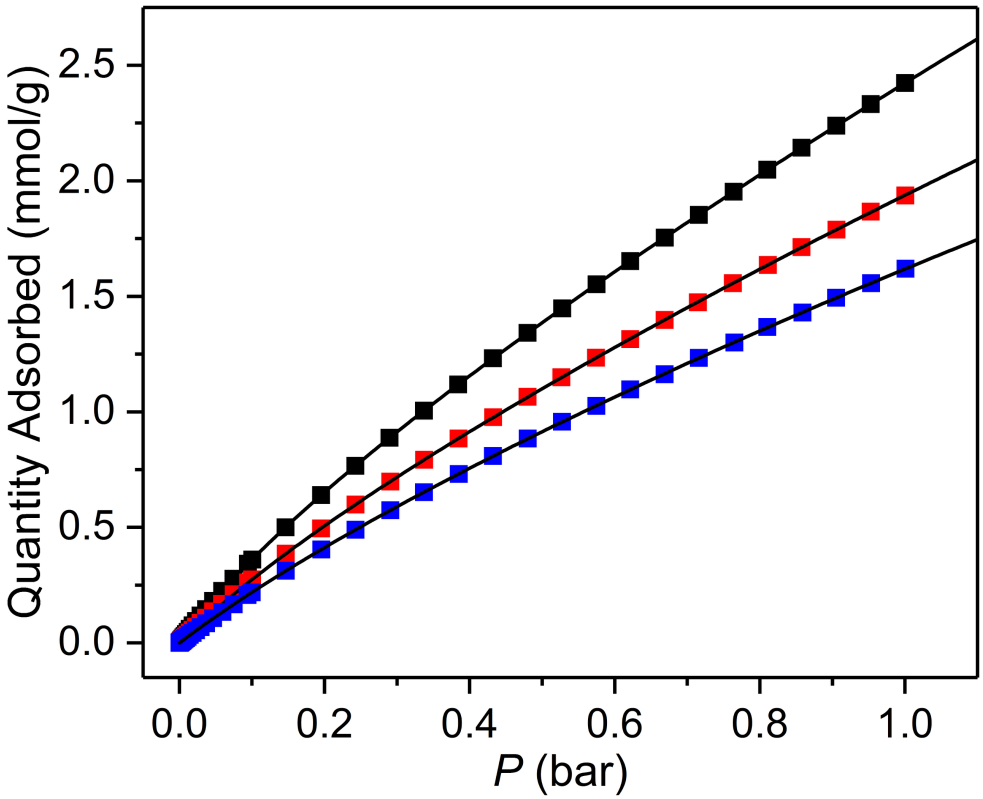

Figure S25. Pure component isotherms data for ethane in Co_bdc_dabco. The black circles refer to 298 K, red for 308 K, and blue for 318 K. The closed circles show adsorption data while the open circles show desorption. The black lines are the respective dual-site Langmuir-Freundlich fits using the parameters in Table S7.

Table S7.

	298 K	**308 K**	**318 K**
$q_{sat,1}$	22.613 ± 27.901	18.084 ± 87.518	11.837 ± 50.053
b_1	0.099 ± 0.097	0.097 ± 0.292	0.131 ± 0.216
v_1	1.000 ± 0.319	0.999 ± 1.542	1.010 ± 1.817
$q_{sat,2}$	0.500 ± 1.029	0.468 ± 5.620	0.350 ± 6.449
b_2	3.515 ± 4.119	2.415 ± 14.375	2.307 ± 21.058
v_2	0.959 ± 0.214	0.953 ± 1.189	0.969 ± 1.837

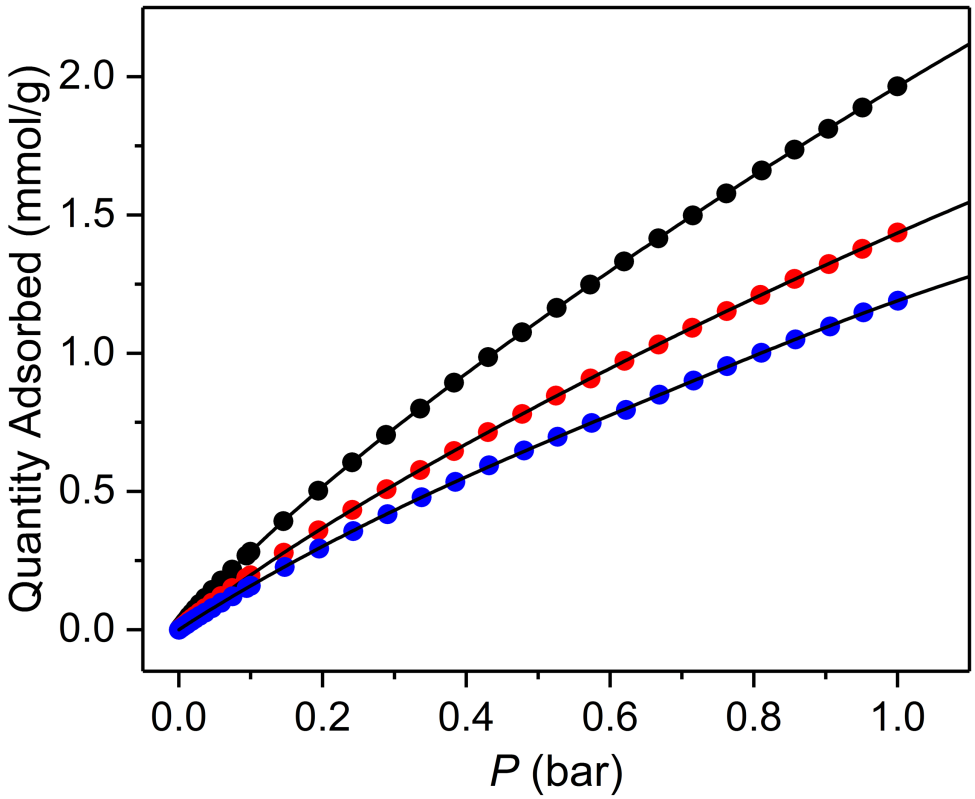

Figure S26. Pure component isotherms data for ethylene in Co_bdc_dabco. The black circles refer to 298 K, red for 308 K, and blue for 318 K. The closed circles show adsorption data while the open circles show desorption. The black lines are the respective dual-site Langmuir-Freundlich fits using the parameters in Table S8.

Table S8.

	298 K	**308 K**	**318 K**
$q_{sat,1}$	3.943 ± 4.169	2.222 ± 5.886	3.921 ± 0.448
b_1	0.238 ± 0.054	0.246 ± 0.076	0.402 ± 0.056
v_1	1.669 ± 0.638	1.765 ± 1.429	0.977 ± 0.009
$q_{sat,2}$	2.328 ± 2.266	2.203 ± 4.767	0.099 ± 0.042
b_2	1.076 ± 0.930	0.827 ± 1.657	2.013 ± 1.046
v_2	0.927 ± 0.017	0.945 ± 0.027	6.245 ± 1.446

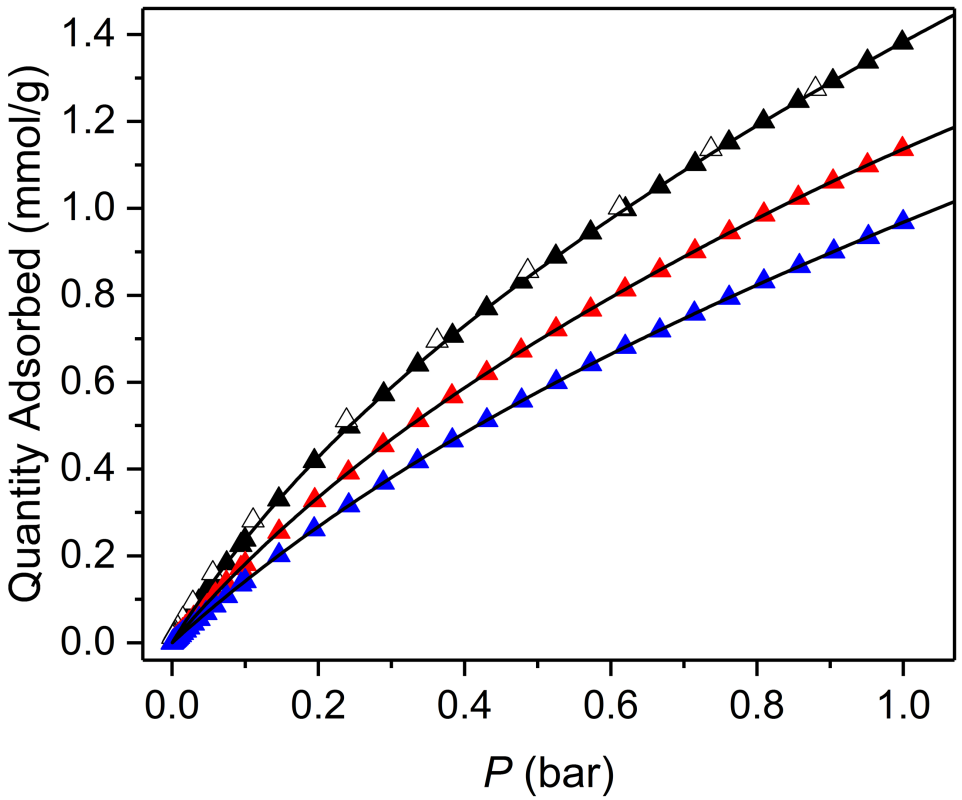

Figure S27. Pure component isotherm data for carbon dioxide in Cu_bdc_dabco. The black triangles refer to 298 K, red for 308 K, and blue for 318 K. The closed triangles show adsorption data while the open triangles show desorption. The black lines are the respective dual-site Langmuir-Freundlich fits using the parameters in Table S9.

Table S9.

	298 K	**308 K**	**318 K**
$q_{sat,1}$ (mmol/g)	1.831 ± 0.280	2.414 ± 0.113	2.591 ± 0.171
b_1 (bar)	1.397 ± 0.213	0.783 ± 0.047	0.564 ± 0.044
v_1	0.982 ± 0.002	0.983 ± 0.004	0.988 ± 0.004
$q_{sat,2}$ (mmol/g)	1.534 ± 0.728	0.174 ± 0.056	0.255 ± 0.527
b_2 (bar)	0.259 ± 0.059	0.780 ± 0.208	0.151 ± 0.290
v_2	1.903 ± 0.337	3.658 ± 0.486	3.483 ± 1.378

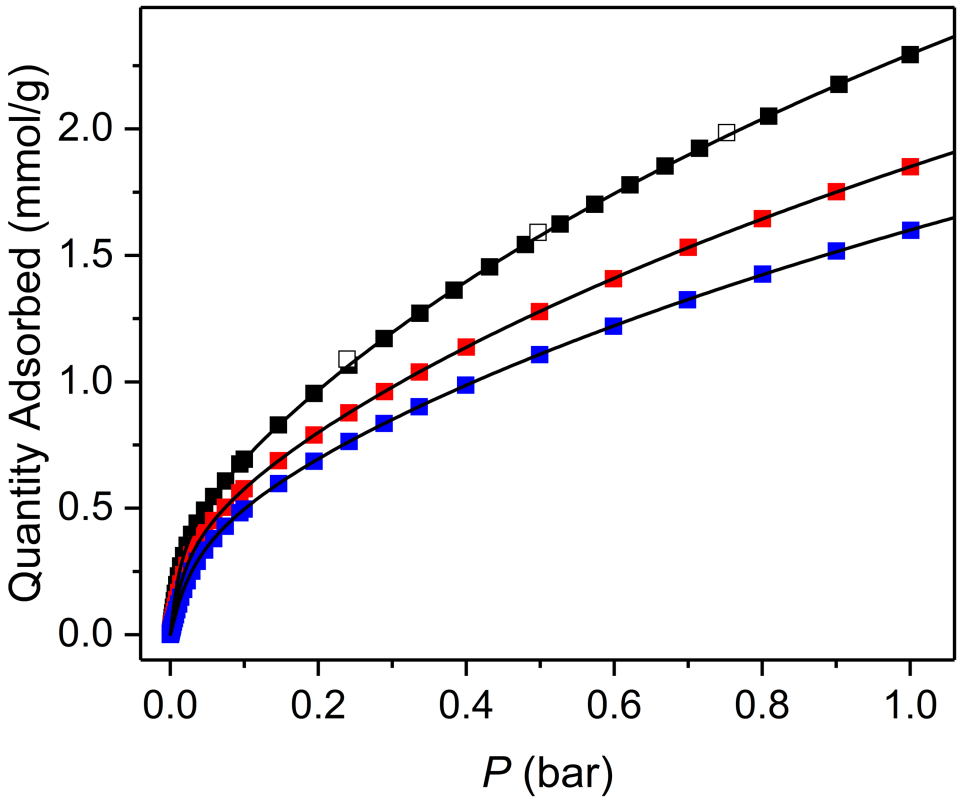

Figure S28. Pure component isotherms data for ethane in Cu_bdc_dabco The black squares refer to 298 K, red for 308 K, and blue for 318 K. The closed sqares show adsorption data while the open squares show desorption. The black lines are the respective single-site Langmuir-Freundlich fits using the parameters in Table S10.

Table S10.

	298 K	**308 K**	**318 K**
$q_{sat,1}$ (mmol/g)	6.969 ± 0.304	7.259 ± 0.285	5.417 ± 0.457
b_1 (bar)	0.382 ± 0.020	0.268 ± 0.012	0.306 ± 0.028
v_1	0.860 ± 0.014	0.804 ± 0.010	0.852 ± 0.027
$q_{sat,2}$ (mmol/g)	0.371 ± 0.011	0.320 ± 0.008	0.335 ± 0.021
b_2 (bar)	194.486 ± 21.802	124.978 ± 9.353	64.709 ± 9.529
v_2	1.195 ± 0.018	0.804 ± 0.014	1.168 ± 0.029

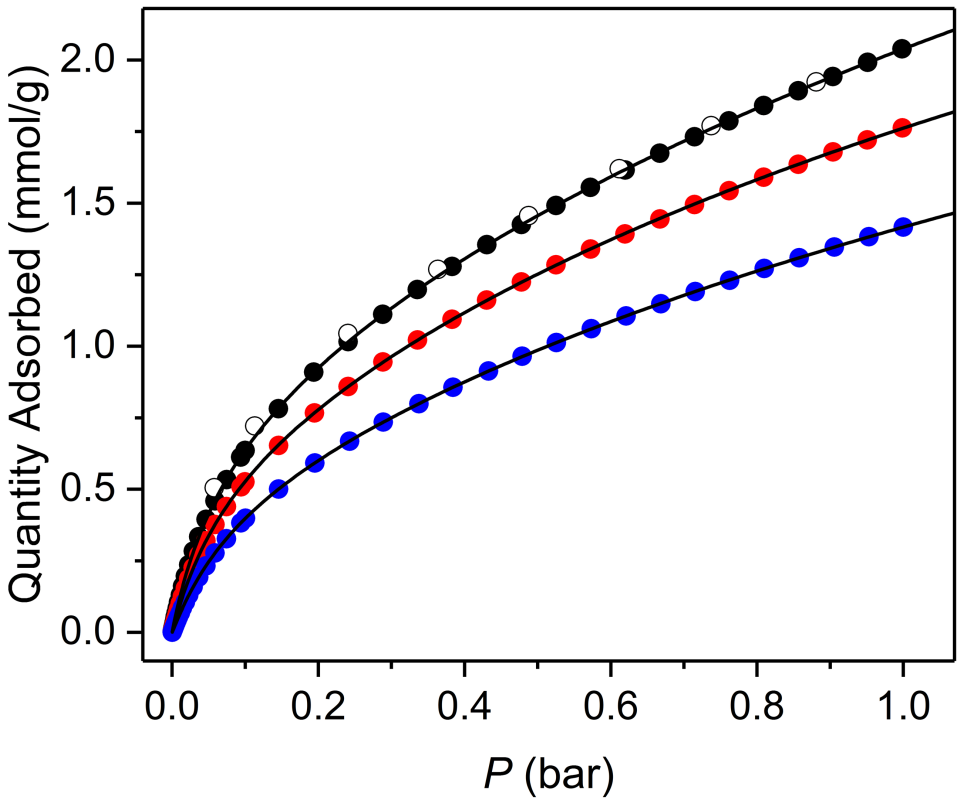

Figure S29. Pure component isotherms data for ethylene in Cu_bdc_dabco The black circles refer to 298 K, red for 308 K, and blue for 318 K. The closed circles show adsorption data while the open circles show desorption. The black lines are the respective single-site Langmuir-Freundlich fits using the parameters in Table S11.

Table S11.

	298 K	**308 K**	**318 K**
$q_{sat,1}$ (mmol/g)	5.713 ± 1.999	4.481 ± 0.513	4.113 ± 0.255
b_1 (bar)	0.315 ± 0.086	0.405 ± 0.032	0.338 ± 0.015
v_1	0.891 ± 0.155	0.881 ± 0.061	0.897 ± 0.031
$q_{sat,2}$ (mmol/g)	0.721 ± 0.231	0.498 ± 0.092	0.399 ± 0.079
b_2 (bar)	13.179 ± 4.730	17.191 ± 4.211	16.694 ± 2.179
v_2	0.987 ± 0.065	1.050 ± 0.049	1.094 ± 0.028

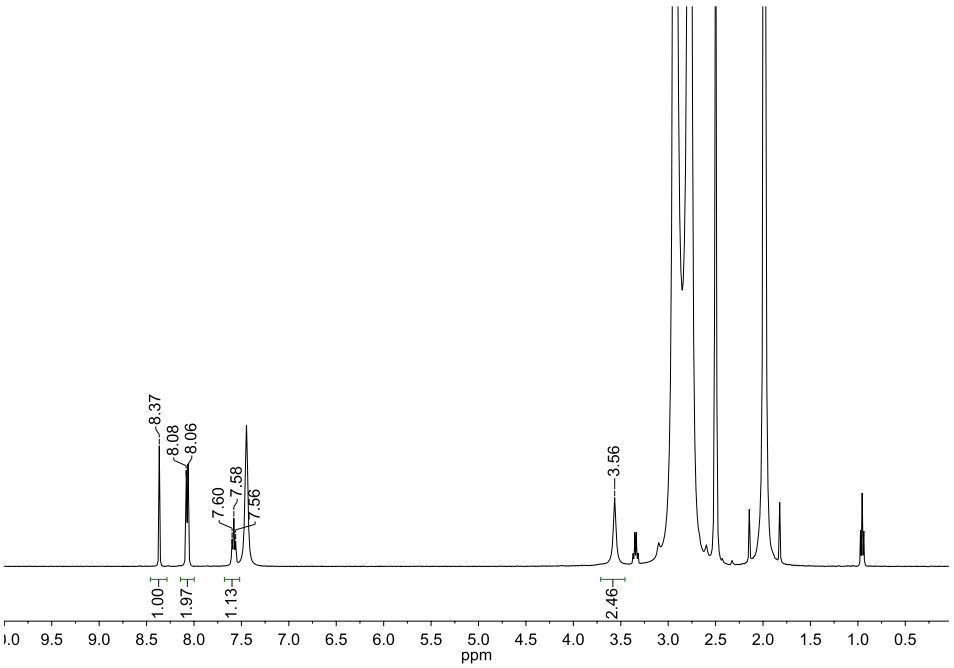

Figure S30. Full ^{1}H-NMR of digested Cu_bdc_dabco. The peaks at centered at 8.37, 8.07, and 7.58 ppm correspond to H_2bdc while the peak at 3.56 is dabco. The broad just below 7.5 ppm is H_2O (acidic conditions) and the remaining peaks correspond to solvent (DMSO-d_5, DMA, and diethyl ether).

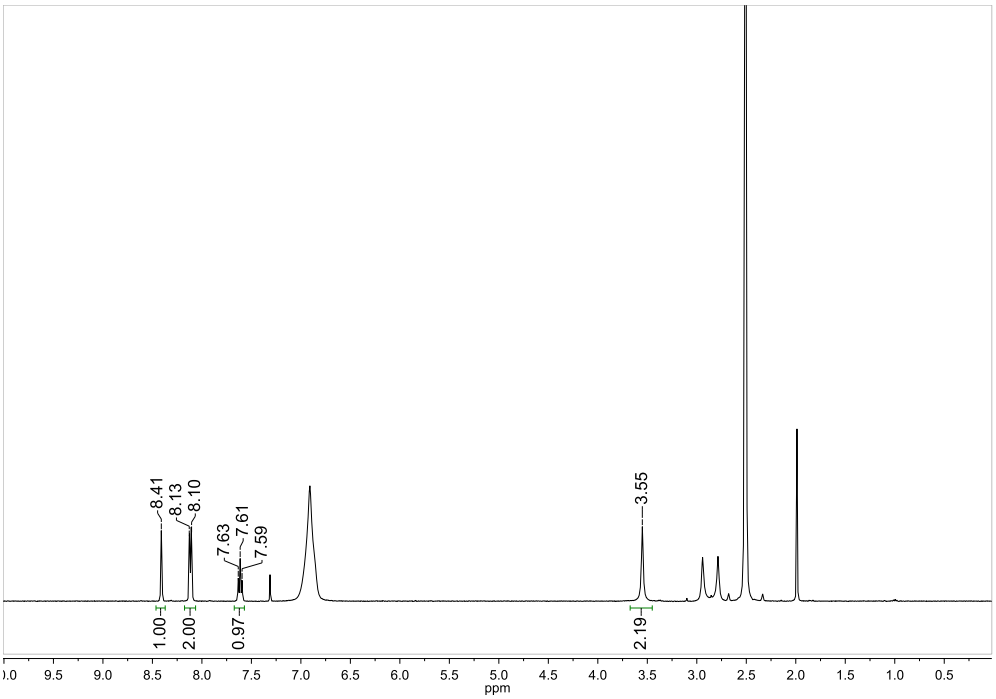

Figure S31. Full ^{1}H-NMR of digested Cu_bdc_dabco$_{0.75}$ The peaks at centered at 8.41, 8.11, and 7.61 ppm correspond to H_2bdc while the peak at 3.55 is dabco. The broad just below 7.0 ppm is H_2O (acidic conditions) and the remaining peaks correspond to solvent (DMSO-d_5, DMA, and chloroform).

References:

1) A. Coelho, Topas Academic v6, Coelho Softw., 2017. http://www.topas-academic.net/
2) H. Chun, H. Jung, Seo, J. *Inorg. Chem.*, 2009, **48**, 2043–2047.
3) G. S. Pawley, Unit-Cell Refinement From Powder Diffraction Scans, *J. Appl. Cryst.*, 1981, **14**, 357–361. https://inis.iaea.org/search/search.aspx?orig_q=RN:13670039.
4) Y. G. Andreev, G. S. MacGlashan, P. G. Bruce, *Phys. Rev. B.*, 1997, **55**, 12011–12017.
5) W. Gee, L. Cadman, H. Hamzah, M. Mahon, P. Raithby, A. Burrows, *Inorg. Chem.*, 2016, **55**, 10839–10842.
6) S. J. Geier, J. A. Mason, E. D. Bloch, W. L. Queen, M. R. Hudson, C. M. Brown, J. R. Long, *Chem. Sci.*, 2013, **4**, 2054-2061.